2022 IEEE/SICE International Symposium on System Integration (SII)
January 9-12, 2022. Narvik, Norway

2022 IEEE/SICE International Symposium on System Integration (SII) | 978-1-6654-4540-5/22/$31.00 ©2022 IEEE | DOI: 10.1109/SII52469.2022.9708894

# Lessons Learned from On-orbit Gyroscope Malfunction and Recovery Operation of Microsatellite RISESAT

Shinya Fujita, Toshinori Kuwahara, Kazuki Kibune, Naoya Shiraishi, Yuji Sato, Yuji Sakamoto, and Junichi Kurihara

***Abstract*— The 50-kg-class Earth observation satellite "RISESAT" is a microsatellite developed mainly by Tohoku University and Hokkaido University, and was successfully launched into orbit by the Epsilon Launch Vehicle No. 4 on January 18, 2019. However, on June 11, 2019, about five months after launch, the three-axis fiber-optic gyroscope (FOG) for attitude control experienced a malfunction, making angular velocity measurement around the satellite's Z-axis unavailable. In this paper, we report our lessons learned on how to solve the single-axis failure of the FOG, which was not expected when RISESAT was developed, by combining the existing functions of the attitude control software. Due to the failure of the FOG, experiments that require high attitude control accuracy, such as high-resolution multispectral observation and laser communication, are now impossible. However, valuable observations such as oceanographic observations and on-orbit monitoring of the radiation environment are still being carried out on a daily basis as of September 2021, more than two years after launch.**

## I. Introduction

The Space Robotics Laboratory (SRL) at Tohoku University and the Space Mission Center at Hokkaido University have been working on the development of 50 kg-class Earth observation satellites for more than 10 years. RISESAT, the fifth in our series of Earth observation satellites, was successfully launched on January 18, 2019, by the Epsilon Launch Vehicle No. 4 with the support of Innovative Satellite Technology Demonstration Program-1 provide by Japan Aerospace Exploration Agency (JAXA). The system specifications are shown in TABLE I and the appearance is shown in Fig. 1.

TABLE I RISESAT System Specification.

| | |
|---|---|
| Dimensions | 500 × 500 × 500 mm |
| Mass | 59.2 kg |
| Orbit | Sun Synchronous Orbit, 500 ± 20 km |
| | LTDN = 9:30 AM |
| Attitude Control | 3-axis and Spin Stabilization |
| | < 0.1° (3σ) (Req.), < 0.04° (Obj.) |
| Power | GaAs Multi. Cell, > 100 W |
| | NiMH, 7.4 Ah, 10.8 V |
| Payloads | High-Precision Telescope (HPT) |
| | Dual-band Optical Transient Camera (DOTCam) |
| | Ocean Observation Camera (OOC) |
| | Space Radiation Micro-Tracker (RISEPix) |
| | Store & Forward Data Packet Decoder (DPD) |
| | De-Orbit Mechanism (DOM) |
| | Micro Monitor Camera (MMC) |
| | Very Small Optical Transmitter (VSOTA) |
| | Corner-Cube Reflector (CCR) |
| Communication | Uplink: UHF 1200 bps, S-band ≤ 4 kbps |
| | HK downlink: S-band, ≤ 500 kbps |
| | Mission Data downlink: X-band, ≤ 2.4 Mbps |

The name "RISESAT" comes from the acronym for "Rapid International Scientific Experiment Satellite", and was developed to carry a variety of scientific instruments developed all over the world to observe the Earth's surface, the near-Earth space environment, and deep space such as planets. Among them, the core mission was high-resolution multispectral observation using HPT (High-Precision Telescope) with LCTF (Liquid Crystal Tunable Filters) (Fig. 2) developed by Hokkaido University. This system allows us to select up to 48 bands from 630 bands in the visible to near-infrared region and to observe with a ground resolution of 3.7 m [1][2].

However, on June 11, 2019, approximately five months after launch, the three-axis fiber-optic gyroscope (FOG) for attitude control experienced a malfunction, making angular velocity measurement around the satellite's Z-axis unavailable. As a result of the manufacturer's investigation into the cause, it was concluded that the problem was caused by a permanent failure of electronic components inside the sensor, and the sensor was considered unlikely to recover. Since the FOG was the only angular velocity sensor equipped with RISESAT, it was fatal for the satellite's attitude control system. The FOG was considered to have a low risk of failure within the RISESAT development team, as it had been used in multiple projects within SRL and at other universities. Various functions to improve the accuracy of the satellite's attitude control were designed to rely on the angular velocity information measured by the FOG, therefore even the minimum attitude control for X-band communication with the ground station was threatened, not to mention the execution of the observation mission.

In this paper, we describe a method to recover the three-axis attitude control capability of approximately 1° by combining the "hidden" function of the attitude control software to solve with the single-axis failure of FOG, which was not assumed during the development of RISESAT. These

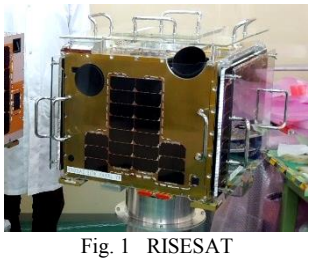

Fig. 1 RISESAT

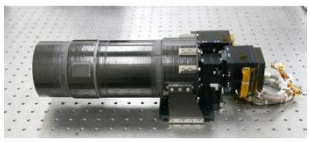

Fig. 2 HPT

S. Fujita, T. Kuwahara, K. Kibune, N. Shiraishi and Y. Sato are with the Department of Aerospace Engineering, Tohoku University, Sendai, Japan (phone: +81-22-795-5082; e-mail: {shinya.fujita.a2, toshinori.kuwahara.b3, kazuki.kibune.p2, naoya.shiraishi.p6, yuji.sato.b4} @tohoku.ac.jp)
Y. Sakamoto is with the Faculty of Engineering, Hokkaido University, Sapporo, Japan (e-mail: yuji.sakamoto@eng.hokudai.ac.jp)
J. Kurihara is with the Faculty of Science, Hokkaido University, Japan; (e-mail: kurihara@sci.hokudai.ac.jp)

measures allowed RISESAT to perform regular ocean color observations using the OOC (Ocean Observation Camera), monitor the on-orbit radiation environment using RISEPix[3], conduct ground-based laser ranging using a corner-cube reflector (CCR)[4], and 2.4 Mbps mission data downlink using the X-band transmitter. Especially in ocean observation, more than 6,000 images have been taken as of September 2021[5].

## II. Attitude Control System of RISESAT

### A. Hardware Architecture

The nine attitude control modes of RISESAT and the transition diagram between the modes are shown in Fig. 3. The attitude control equipment used in each mode is shown in Fig. 4. The attitude control mode of RISESAT can be classified into coarse attitude control and fine attitude control. The fine attitude control modes include the ground point tracking mode used for multispectral observation, optical communication and high-speed X-band communication, the inertial pointing mode and planet pointing mode used for astronomical observation, the local horizontal and vertical system (LVLH) mode for ocean observation. RISESAT also has two deployable solar panels that can generate up to about 100 W by orienting them toward the Sun.

The hardware block diagram of the attitude control system is shown in Fig. 5. Attitude Control Unit (ACU) is a Field-Programmable Gate Array (FPGA) based computer, and an OpenRISC1200 32bit softcore processor developed by OpenCore.org is integrated. The advantage of the FPGA-based

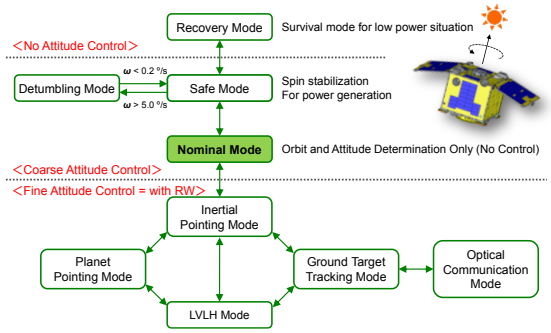


Fig. 3 Attitude Modes and Its Transition Diagram of RISESAT.

| # | Mode | GPSR | GAS | SAS | SES | FOG | STT | MTQ | RW | ACU | ACUS |
|---|---|---|---|---|---|---|---|---|---|---|---|
| 1 | Recovery | | | | | | | | | | |
| 2 | Detumbling | | ○ | | | | | ○ | | | |
| 3 | Safe | | ○ | ○ | | | | ○ | | ○ | |
| 4 | Nominal | ○ | ○ | ○ | | ○ | | ○ | ○ | ○ | |
| 5 | Inertial Pointing | ○ | ○ | ○ | ○ | ○ | ○ | | ○ | ○ | ○ |
| 6 | LVLH | ○ | ○ | ○ | ○ | ○ | ○ | | ○ | ○ | ○ |
| 7 | Planet Pointing | ○ | ○ | ○ | ○ | ○ | ○ | | ○ | ○ | ○ |
| 8 | Ground Target Tracking | ○ | ○ | | | ○ | | | ○ | ○ | ○ |
| 9 | Optical Communication | ○ | ○ | | | ○ | | | ○ | ○ | ○ |

Fig. 4 The Attitude Control Equipment Used in Each Mode.

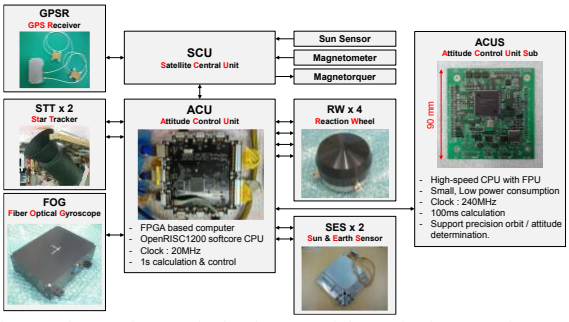


Fig. 5 The Hardware Block Diagram of the Attitude Control System.

ACU is that it can communicate with multiple sensors simultaneously, but mathematical calculations are slow due to the low operating frequency of 20 MHz and the lack of an FPU. Therefore, we added ACUS, which specializes in computing higher-order environmental models and performing filter processing of sensor data. For the ACUS, we used a 32-bit microcontroller (RX71M, Renesas) with a built-in FPU running at 240 MHz, which can perform numerical calculations more than 1000 times faster than the ACU [6].

Two Star Trackers (STTs) were collaboratively developed by Tohoku University and Meisei Electric Co. SRL has been developing its own STT since the launch of the 50-kg-class satellite RISING-2 in 2014, and this STT is the third generation [7]. The results of the on-orbit demonstration show that this STT has an attitude determination accuracy of 0.6° (3σ) around boresight and 0.06° (3σ) around cross-boresight, but it cannot be used when the angular velocity of the satellite exceeds 0.3°/s. Though the STT is equipped with a baffle for light shielding, it is essential to maintain an Earth incidence angle of 120° or more, a sun incidence angle of 80° or more, and a Moon incidence angle of 30° or more relative to the STT optical axis for stable star identification.

The Sun and Earth Sensor (SES) is a sensor unit developed in SRL that combines the fine sun sensor and the Earth sensor into a single unit. Two SESs are mounted on top of the satellite to provide a hemispheric field of view in the zenith direction. The previous generation of our fine sun sensor was designed to measure the direction of sunlight incidence by using a linear PSD (Position Sensitive Detector), but the measurement accuracy was insufficient because the effect of albedo light could not be excluded. The new model installed in RISESAT uses a 256-pixel linear CMOS sensor that can distinguish between sunlight and albedo light depending on the angular diameter of the light source. The Earth Sensor is a sensor that detects the temperature difference between the cosmic microwave background radiation of about 3 K and the Earth's temperature of about 300 K using thermopiles [8]. The Earth sensor of RISESAT is only intended to verify thermopile technology and does not have the capability to autonomously determine the Earth direction on orbit.

### B. Software Architecture

RISESAT has the capability to perform orbit and attitude determination, attitude guidance and control autonomously without ground support. A brief block diagram of the software is shown in Fig. 6. The ACU divides the feedback control of a one-second cycle into 100 ms subroutines SR0 to SR9 and executes them. The control cycle is triggered by the PPS signal from the GPSR, which is synchronized to the UTC seconds. By dividing the processing every 100 ms, the timing of receiving data from the sensor and sending commands to the actuator can be kept constant even when the computational load varies according to the control task.

In SR0, which is executed immediately after the detection of the PPS signal, time management of the ACU and physical quantity conversion of data received from various sensors are executed. The ACU internally manages three time standards, UTC, which is synchronized with GPS system, UT1 and TT, which are necessary for the calculation of environmental models. The time difference information between UTC and UT1 and between UTC and TT cannot be obtained within the ACU, so the values released by the International Earth

Rotation Satellite (IERS) must be uploaded daily by commands from the ground.

In the following SR1, the IAU 1980 Earth nutation model is calculated based on the updated time information. The original model has 106th-order, but we limited it to 10th-order because the ACU cannot finish the process within 100 ms.

In SR2, the IAU 1976 Earth precession model, the IAU 1982 Earth rotation model, and the IERS 1996 polar motion model are calculated, and orbit estimation using GPS is performed. GPSR provides two seconds old positioning information in the WGS84 coordinate system at SR0. After transforming the position vector in the WGS84 geodetic coordinate system to the position vector in the GCRS inertial coordinate system two seconds ago, the satellite position and velocity at the current time are estimated.

In SR3, we calculate the geomagnetic field model using IGRF-12. The geomagnetic field model calculation is the most time-consuming process performed by the ACU, taking several seconds to several tens of seconds to execute in stages. The frequency of updating the geomagnetic field vectors varies with the specified model order. While the geomagnetic field model values are not updated, linear interpolation is used to reduce the error.

In SR4, inertial navigation calculation is performed by integrating the angular velocity obtained from the FOG. The angular velocity data is sampled at 10 Hz, and is always prepared to provide relative attitude changes based on the attitude immediately after the FOG startup.

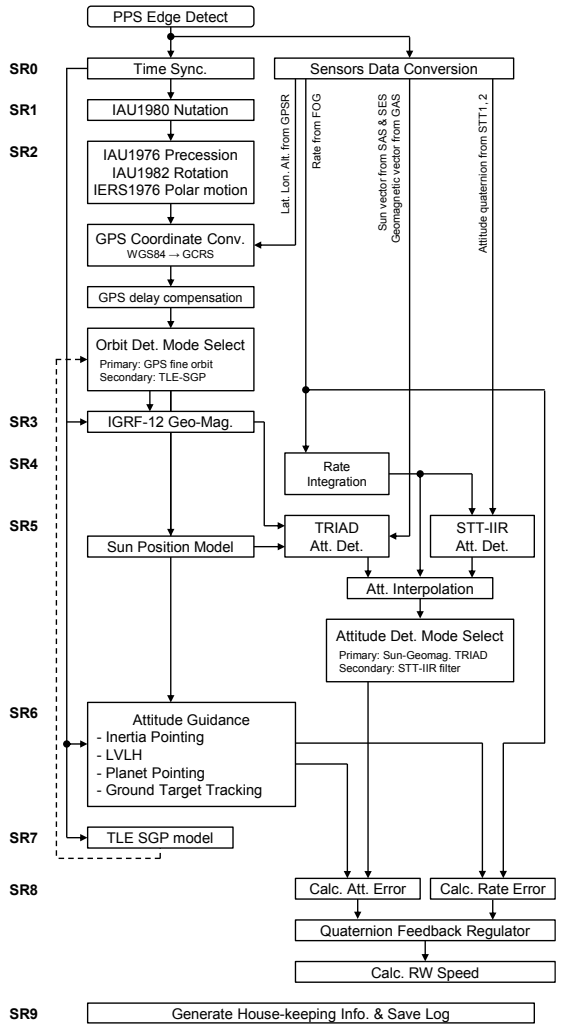

Fig. 6 A Brief Block Diagram of the Attitude Control Software.

In SR5, the sun position calculation and attitude determination are performed. RISESAT can provide coarse attitude using the TRIAD method based on sun sensor and geomagnetic sensor, and fine attitude using two STTs. In the case of STT attitude determination with IIR filter, it is possible to determine the attitude within 0.05° (3σ) accuracy, but there are many restrictions on its use, such as the upper limit of angular velocity and boresight direction of STT optics[10]. Therefore, a coarse attitude determination system is required to guide the satellite to an attitude where STTs are available in advance. If a sensor error occurs in the STT while using the fine attitude determination system, the system has a function to automatically estimate the current attitude based on the attitude at the time when it was normal at the last time, using the relative attitude change calculated in SR4.

In SR6, the target attitude is calculated according to the various attitude control modes. The target attitude is given in quaternions, and the target angular velocity is obtained by its derivative.

In SR7, the Two-Line Elements (TLE) uploaded from the ground is processed by the SGP algorithm and converted into position and velocity in the GCRS coordinate system. The orbit determination results obtained here will be used in SR2 of the next attitude control cycle.

In SR8, the amount of control to the target attitude is calculated. Integrate the target control torque and set the target speed every second for reaction wheels (RWs).

In SR9, the status of the ACU is summarized into 1440 bytes of telemetry information and sent to the SCU, the main computer of the satellite. The ACU status during the time when the satellite is invisible can be logged to a 2 Mbyte SRAM at regular intervals. If the data is saved every second, the log can be kept for 1365 s, and the maximum recording interval is 255 s. Communication with various sensors and actuators is running constantly in the background using the FPGA, and commands from the ground station are received and processed between each subroutine. RISESAT does not have the capability to remotely update its software after launch.

## III. Recovery of Three-Axis Angular Velocity Determination Function after the FOG Malfunction

On June 11, 2019, about five months after launch, the three-axis FOG experienced a malfunction, making angular velocity measurement around the satellite's Z-axis unavailable. The angular velocity measured on June 14 after the malfunction occurred is shown in Fig. 7. We can find that the output value of the angular velocity around Z-axis is apparently smaller than the angular velocity around X and Y axes. This was also consistent with the abnormal current of Z-axis sensor circuit indicated by the self-diagnosis function of the FOG. As a result of verification by the manufacturer, it was identified that the malfunction was caused by accidental and permanent failure of electronic components inside the sensor, and although the power consumption of the entire FOG increased by about 10 to 20%, it was confirmed that the remaining two axes could continue to be used without spreading the failure to the satellite system.

On the other hand, as shown in the configuration of the attitude control system in the previous chapter, RISESAT does

not have redundant angular velocity sensors, and it was necessary to handle the problem in software to continue operation. One method that does not depend on other sensors is to use the law of conservation of angular momentum. Assuming that the inertia tensor of the satellite is known and there is no external torque, the angular momentum of the entire satellite is conserved, so it is theoretically easy to estimate the angular velocity around the Z-axis from the angular velocity of the two remaining axes. However, since this function is not implemented in the ACU of RISESAT, and there is no function to update software from the ground, this method is not applicable. Therefore, we adopted a method to obtain the angular velocity by differentiating the attitude determination result obtained from the sun sensor and the geomagnetic sensor. RISESAT ACU had a function to differentiate the results of attitude determination so that the angular velocity could be coarsely determined even when FOG was turned off to save power.

Given that $\boldsymbol{q}(t) \in \mathbb{H}$ is the quaternion representing the attitude of the body coordinate system relative to the inertial coordinate system at time $t \in \mathbb{R}$, the attitude change $\Delta\boldsymbol{q} \in \mathbb{H}$ until after $\Delta t \in \mathbb{R}$ is represented by (1). Here $\otimes$ is the Hamiltonian product. If the vector part of $\Delta\boldsymbol{q}$ is $\Delta\boldsymbol{q}_{\mathrm{v}}v$ and the scalar part is $\Delta q_{\mathrm{s}}$, the average angular velocity $\boldsymbol{\omega}$ during $\Delta t$ can be expressed as (2).

$$\Delta\boldsymbol{q} = \boldsymbol{q}(t)^{-1} \otimes \boldsymbol{q}(t + \Delta t) \tag{1}$$

$$\boldsymbol{\omega} = \frac{2\cos^{-1}(\Delta q_{\mathrm{s}})}{\Delta t}\Delta\boldsymbol{q}_{\mathrm{v}} \tag{2}$$

In RISESAT, $\Delta t$ is 10 s and this function is available only in the sunshine region where the sun sensor is available. Originally, this function was designed to be used when FOG was turned off, so it was not possible to combine the use of

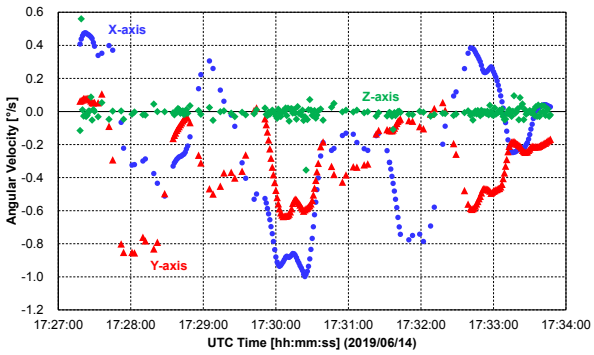


Fig. 7 Angular Velocity Measurement after the FOG Malfunction.

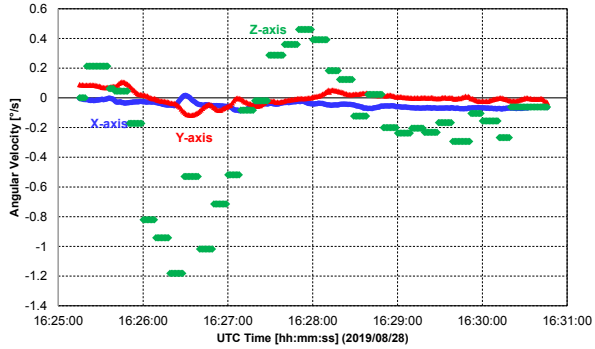


Fig. 8 Angular Velocity when FOG-XY Axis Measurements and Attitude Derivative Values are Combined.

FOG output values only for the XY-axis and attitude derivative values only for the Z-axis. Therefore, by setting the attitude derivative as the angular velocity bias of FOG, those results were merged onboard. The bias compensation value was a variable that was supposed to be set by command from the ground station. The copying function between global variables, which was included as a debugging function during ACU software development, is used to copy the value of the 32-bit float written to the address of the attitude derivative Z-axis component every 2 s to the address of the bias compensation variable. The results of the three-axis angular velocity determination when this measure is applied are shown in Fig. 8. Since the angular velocity around the Z-axis is only updated every 10 s, the estimated values are stepwise, however, it can be seen that the overall trend can be obtained.

Based on the lessons learned, SRL's microsatellites developed after RISESAT is equipped with an on-orbit software update function to deal with unexpected problems.

## IV. Restoration of the Three-Axis Attitude Control

Consider conducting three-axis attitude control using RWs, although the update frequency of angular velocity measurement around the Z-axis has been reduced to 1/10 of the other axes. In RISESAT, the Quaternion Feedback Regulator (3) proposed by Wie et al. is used as the attitude control law, and the proportional gain $\boldsymbol{k}_{\mathrm{P}} \in \mathbb{R}^3$ and the derivative gain $\boldsymbol{k}_{\mathrm{D}} \in \mathbb{R}^3$ of the three axes can be set independently[10]. In (3), $\boldsymbol{T}_{\mathrm{d}} \in \mathbb{R}^3$ is the desired control torque vector input to the RWs, $\boldsymbol{\omega}_{\mathrm{e}} \in \mathbb{R}^3$ is the angular velocity error vector, $\boldsymbol{q}_{\mathrm{e}} \in \mathbb{R}^3$ is the vector part of the attitude error quaternion, $\boldsymbol{\omega}_{\mathrm{b}} \in \mathbb{R}^3$ is the current angular velocity vector of the satellite, $\boldsymbol{J} \in \mathbb{R}^{3\times3}$ is the satellite inertia tensor, and $\boldsymbol{h}_{\mathrm{w}} \in \mathbb{R}^3$ is the angular momentum vector of the RWs.

$$\boldsymbol{T}_{\mathrm{d}} = -\boldsymbol{k}_{\mathrm{D}}\boldsymbol{\omega}_{\mathrm{e}} - \boldsymbol{k}_{P}\boldsymbol{q}_{\mathrm{e}} - \boldsymbol{\omega}_{\mathrm{b}} \times (\boldsymbol{J}\boldsymbol{\omega}_{\mathrm{b}} + \boldsymbol{h}_{\mathrm{w}}) \tag{3}$$

Attitude control experiments by changing the control gain around the Z axis were conducted on the orbit. The four combinations of gain settings that we experimented with are shown in TABLE III. The experiment was conducted from August 6 to 9, 2019.

The change in the Z-axis component of the control error is shown in Fig. 9. Due to the nature of on-orbit experiments, the initial conditions are not standardized, but the elapsed time from the start of attitude control is consistent. In order to reduce the coupling of the control around the Z axis on the control of the other two axes, only the X and Y axes are controlled first to point the satellite Z-axis direction to nadir, and then the control of Z-axis is started.

Pattern #1 with normal gain setting shows that the error oscillates sinusoidally while the amplitude increases, indicating that the control has failed. The remaining patterns #2 - #4 are those where only the Z-axis gain is reduced by a certain ratio. From these results, it was confirmed that 1/10 gain was too long to converge, 2/5 gain did not converge, and 1/5 of the original control gain was effective for practical use.

We applied the results of this experiment and verified the effectiveness of the measures through Earth observation experiments using the OOC. The OOC is an observation instrument developed mainly by the Space Mission Center of Hokkaido University, and was designed to measure colored

dissolved organic matter (CDOM) in seawater. Although its ground resolution is lower than that of the HPT at 74 m, it can take images in the 405 nm band, which cannot be observed by the HPT, and provides the world's highest resolution as a camera for ocean observation, including that of large satellites. In order to observe a wide area, the push frame method is used, which takes images at regular time intervals while the satellite is fixed in LVLH mode.

To validate the control results, the OOC (5.5° field of view) was pointed around Denver, Colorado, USA, and the observation was performed as shown in Fig. 11. The principal axis of the OOC is mounted approximately parallel to the satellite Z-axis. The results showed that those 10 images were continuously oriented in the same direction, confirming that this emergency attitude control around the Z-axis is effective in practical use. This attitude control is also used for the radiometric calibration of the OOC with the Moon, which contributes to the evaluation of CCDs in orbit[10][11].

## V. Two-Axis Ground Target Tracking Control

Although RISESAT has recovered LVLH attitude control with a control accuracy of less than 1° by the measures in the previous chapter, an X-band transmitter with a data rate of 2.4 Mbps is required to downlink the large amount of data observed by the OOC. Since the X-band antenna (XANT) has a narrow beam width, it is necessary to track the ground station direction using ground target tracking control (required pointing accuracy < 10°). This technology can also be used for satellite laser ranging (SLR) experiments using the CCR on RISESAT. Since the satellite tracks a relatively moving target, it is difficult to deal with it by reducing the gain of the control around the Z-axis as proposed earlier. Fortunately, both XANT and CCR have symmetrical characteristics around the satellite Z-axis, so the angle of rotation around the Z-axis with respect to the ground station was not important. Therefore, it was required to create a two-axis target pointing control system using only the X and Y axes.

TABLE III Combinations of Control Gains in the Experiments.

| # | $\boldsymbol{k}_\mathrm{P}$ | $\boldsymbol{k}_\mathrm{D}$ |
|---|---|---|
| 1 | [0.05 0.05 0.05] | [0.8 0.8 0.8] |
| 2 | [0.05 0.05 0.005] | [0.8 0.8 0.08] |
| 3 | [0.05 0.05 0.01] | [0.8 0.8 0.16] |
| 4 | [0.05 0.05 0.02] | [0.8 0.8 0.32] |

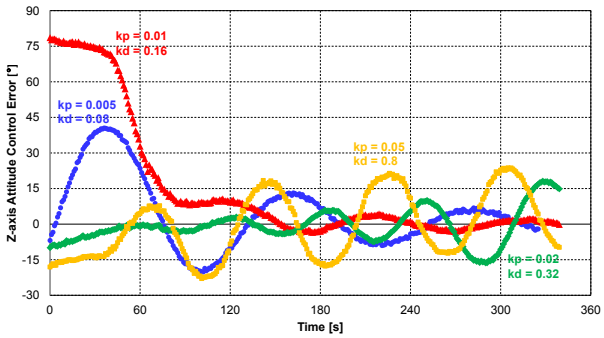


Fig. 9 Z-axis Component of Attitude Control Error in each Control Gain.

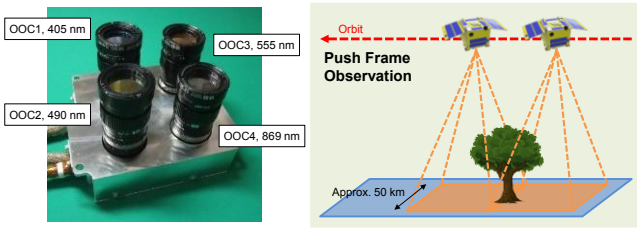


Fig. 10 OOC and Push-Frame Observation Method.

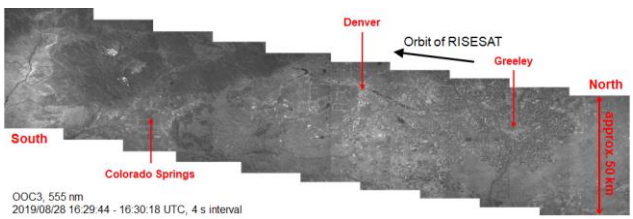


Fig. 11 Sequential Image around Denver Taken by OOC.

RISESAT implemented several guidance laws for target tracking control, and one of them was a guidance law that transfers from an arbitrary reference attitude to target tracking attitude with the shortest maneuver angle. This was implemented in order to change from the inertial pointing mode attitude where a STT can be used to the target tracking mode attitude in the shortest possible time by not rotating around the Z-axis, which is also unconstrained in HPT observations[13].

When the satellite Z-axis is directed to the ground target without causing rotation around the satellite Z-axis from the reference attitude $\boldsymbol{q}_\mathrm{i}^\mathrm{ref} \in \mathbb{H}$ defined in the Earth Centered Inertial (ECI) coordinate system, the target attitude quaternion $\boldsymbol{q}_\mathrm{i}^\mathrm{d} \in \mathbb{H}$ is obtained by (4). Here, $\boldsymbol{e}_\mathrm{z,b} \in \boldsymbol{S}^2$ is the basis vector representing its Z-axis in the body coordinate system, $\boldsymbol{R}_\mathrm{i} \in \mathbb{R}^3$ is the position vector of the target point on Earth in the ECI frame, and $\boldsymbol{r}_\mathrm{i} \in \mathbb{R}^3$ is the position vector of the satellite in the ECI frame.

$$\boldsymbol{e}_\mathrm{z,i} = \boldsymbol{q}_\mathrm{i}^{\mathrm{ref}-1} \boldsymbol{e}_\mathrm{z,b} \boldsymbol{q}_\mathrm{i}^\mathrm{ref} \tag{4}$$

$$\boldsymbol{u}_\mathrm{bore} = \frac{\boldsymbol{R}_\mathrm{i} - \boldsymbol{r}_\mathrm{i}}{\|\boldsymbol{R}_\mathrm{i} - \boldsymbol{r}_\mathrm{i}\|} \tag{5}$$

$$\boldsymbol{q}_\mathrm{ref}^\mathrm{d} = \begin{cases} (\boldsymbol{e}_\mathrm{z,i} \times \boldsymbol{u}_\mathrm{bore}) \sin^{-1}\left(\dfrac{\boldsymbol{e}_\mathrm{z} \cdot \boldsymbol{u}_\mathrm{bore}}{2}\right) \\ \cos^{-1}\left(\dfrac{\boldsymbol{e}_\mathrm{z} \cdot \boldsymbol{u}_\mathrm{bore}}{2}\right) \end{cases} \tag{6}$$

$$\boldsymbol{q}_\mathrm{i}^\mathrm{d} = \boldsymbol{q}_\mathrm{ref}^\mathrm{d}\, \boldsymbol{q}_\mathrm{i}^\mathrm{ref} \tag{7}$$

Using this guidance law and substituting the satellite's current attitude quaternion $\boldsymbol{q}_\mathrm{i}^\mathrm{b} \in \mathbb{H}$ as a substitute for $\boldsymbol{q}_\mathrm{i}^\mathrm{ref}$, the satellite will always start from its current attitude to the target tracking attitude without any Z-axis rotation control. This enables attitude control without using angular rate determination by attitude differentiation. Originally, $\boldsymbol{q}_\mathrm{i}^\mathrm{ref}$ was a value that should be set by a command from a ground station, and RISESAT ACU did not have a function to substitute $\boldsymbol{q}_\mathrm{i}^\mathrm{b}$ automatically. Therefore, as in the previous chapter, the addressable copy function between global variables made a contribution. Ideally, the substitution should be done every 1 s, which is the same as the attitude control cycle. However, since the substitution operation consumes 10 s for three commands and the number of commands that can be

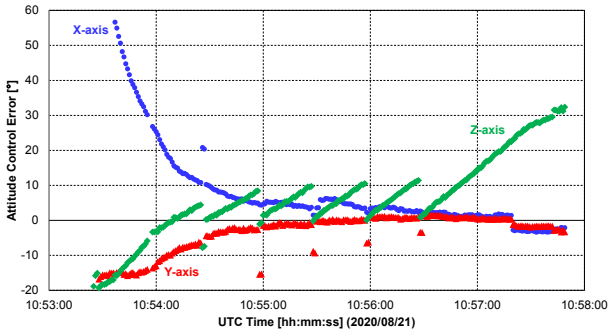


Fig. 12 Example of Attitude Control Error in Two-Axis Ground Target Tracking Control.

registered in the satellite is limited. It was decided to perform this Z-axis rotation control reset operation once every 30 s.

An example of this control in orbit is shown in Fig. 12. The discontinuous sawtooth-like change in the control error around the Z-axis is caused by the fact that the rotation angle error around the Z-axis is reset every 30 s, forcing the error immediately after to zero.

Successor satellites learned the lessons of this case and implemented a function to perform target tracking control using only two axes from the beginning. This function enables control with only two RWs and saves power consumption.

## VI. Conclusion

This paper described an attitude control method to continue operations under the FOG malfunction that occurred approximately five months after the launch of RISESAT.

In RISESAT, the angular velocity output around the satellite Z-axis was permanently disabled due to a malfunction in the electronics inside the FOG. Since RISESAT does not have an on-orbit software update function for the attitude control software, it was required to recover the attitude control function as much as possible by combining existing software functions. To estimate the angular velocity around the Z-axis, we used the attitude differentiation function that was prepared for low power consumption operation. Though the angular velocity can only be obtained in the sunshine region due to the need for a sun vector, a coarse angular velocity can be provided every 10 s.

The function of the three-axis attitude control was recovered by reducing the control gain only around the Z-axis to 1/5 of the normal value. Fixed target attitudes such as inertial pointing mode and LVLH mode can be controlled with an error of less than 1°, contributing to daily observation operations by the OOC.

For the ground target tracking control, which dynamically changes the target attitude, a two-axis attitude control system was constructed using the existing functions. By setting the current attitude as the reference attitude for target tracking control once every 30 s, the error around the Z-axis is forcibly set to zero, and the ground target can be tracked only by controlling the X and Y axes without actively controlling around the Z-axis. Although we could not fulfill the requirement of multispectral observation using the HPT due to the low pointing accuracy of about 10°, we were able to carry out high-speed X-band communication and laser ranging experiments from the ground.

These emergency attitude control functions have been implemented in a more sophisticated form as standard functions in SRL's 50-kg-class microsatellites developed after RISESAT. They also have the ability to update software remotely from the ground to deal with unexpected problems.

## Acknowledgment

This work was supported by JSPS KAKENHI Grant Number JP21K14342. The RISESAT project is supported by Innovative Satellite Technology Demonstration Program of JAXA.

## References

[1] J. Kurihara, Y. Takahashi, Y. Sakamoto, et al., “HPT: A High Spatial Resolution Multispectral Sensor for Microsatellite Remote Sensing”, *Sensors*, Vol.18, No.619, 2018

[2] J. Kurihara, T. Kuwahara, S. Fujita, et al., “A High Spatial Resolution Multispectral Sensor on the RISESAT Microsatellite”, *Trans. of the Japan Society for Aeronautical and Space Science, Aerospace Technology Japan*, Vo.18, No.5, pp. 186–191, 2020

[3] R. Filgas, M. Malich, T. Kuwahara, et al., “RISEPix—A Timepix-based radiation monitor telescope onboard the RISESAT satellite”, *Astronomisch Nachrichten*, Vol. 340, pp. 674–680, 2019

[4] H. Takenaka, H. Kunimori, T. Kuwahara, “Optical Communication Experiment with Microsatellite Body-Pointing using VSOTA on RISESAT”, in *Proc. Advances in Communications Satellite Systems. 37th International Communications Satellite Systems Conference*, Okinawa, Japan, 2019

[5] N. Shiraishi, K. Kibune, S. Fujita, et al., "Automated Mission Planning System for Ocean Observation of Micro-satellite RISESAT," in *Proc. 2021 IEEE/SICE International Symposium on System Integration*, Virtual, pp. 656–661, 2021

[6] S. Fujita, Y. Sato, T. Kuwahara, et al., “On-ground Verification of Attitude Control System for 50-kg-class Microsatellite using a Hardware-in-the-Loop-Simulator”, in *Proc. 68th International Astronautical Congress*, 25-29 September, Adelaide, Australia, pp.6141–6150, 2017

[7] Y. Sato, T. Kuwahara, S. Fujita, et al., “Development and Ground Evaluation of Fast Tracking Algorithm for Star Trackers”, *Trans. of the Japan Society for Aeronautical and Space Science, Aerospace Technology Japan*, Vol. 16, Issue 3, pp. 202–209, 2018

[8] T. Kuwahara, K. Fukuda, N. Sugimura, et al., “Design and Implementation of a Thermopile-Based Earth Sensor”, *Trans. of the Japan Society for Aeronautical and Space Science, Aerospace Technology Japan*, Vol. 14, No.30, Pf_77-Pf_81, 2016

[9] S. Fujita, Y. Sato, T. Kuwahara, et. al., “Development and Ground Evaluation of Ground-Target Tracking Control of Microsatellite RISESAT”, *Trans. of the Japan Society for Aeronautical and Space Science, Aerospace Technology Japan*, Vol. 17, pp. 120–126, 2019

[10] B. Wie and H. Weiss, “Quaternion Feedback Regulator for Spacecraft Eigenaxis Rotations, *J. of Guidance, Control and Dynamics*, Vol. 12, No.3, pp. 375–380, 1989

[11] M. Imai, J. Kurihara, T. Kouyama, et al., "Radiometric Calibration for a Multispectral Sensor Onboard RISESAT Microsatellite Based on Lunar Observations", *Sensors*, Vol.21, No.7, 2021

[12] M. Imai, T. Kouyama, J. Kurihara, et al., “Inflight Radiometric Calibration for a Multi-Band Sensor Onboard Risesat with the Moon”, in Proc. *2020 IEEE International Geoscience and Remote Sensing Symposium*, pp. 6222–6225, 2020

[13] S. Fujita, Y. Sato, T. Kuwahara, et al., “Attitude Maneuvering Sequence Design of High-Precision Ground Target Tracking Control for Multispectral Earth Observations”, in *Proc. 2019 IEEE/SICE International Symposium on System Integration*, Paris, France, pp. 153–158, 2019